Manokaran, V, Michael, AX, Pazhani, A and Batako, A

Residual Stress Evolution of Graphene-Reinforced AA2195 (Aluminum–Lithium) Composite for Aerospace Structural Hydrogen Fuel Tank Application

Journal of
Composites Science

MDPI

Article

Residual Stress Evolution of Graphene-Reinforced AA2195 (Aluminum–Lithium) Composite for Aerospace Structural Hydrogen Fuel Tank Application

Venkatraman Manokaran [1], Anthony Xavior Michael [1,*], Ashwath Pazhani [2,*] and Andre Batako [3]

[1] School of Mechanical Engineering, Vellore Institute of Technology, Vellore 632014, Tamil Nadu, India; venkatraman.m2020@vitstudent.ac.in
[2] Faculty of Engineering, Environment and Computing, Coventry University, Coventry CV1 5FB, UK
[3] General Engineering Research Institute, Liverpool John Moores University (LJMU), Liverpool L3 5UX, UK; a.d.batako@ljmu.ac.uk
* Correspondence: manthonyxavior@vit.ac.in (A.X.M.); ae0255@coventry.ac.uk (A.P.)

Abstract

This study investigates the fabrication and residual stress behavior of a 0.5 wt.% graphene-reinforced AA2195 aluminum matrix composite, developed for advanced aerospace structural applications. The composite was synthesized via squeeze casting, followed by a multi-pass hot rolling process and subsequent T8 heat treatment. The evolution of residual stress was systematically examined after each rolling pass and during thermal treatments. The successful incorporation of graphene into the matrix was confirmed through Energy-Dispersive Spectroscopy (EDS) analysis. Residual stress measurements after each pass revealed a progressive increase in compressive stress, reaching a maximum of −68 MPa after the fourth hot rolling pass. Prior to the fifth pass, a solution treatment at 530 °C was performed to dissolve coarse precipitates and relieve internal stresses. Cold rolling during the fifth pass reduced the compressive residual stress to −40 MPa, and subsequent artificial aging at 180 °C for 48 h further decreased it to −23 MPa due to recovery and stress relaxation mechanisms. Compared to the unreinforced AA2195 alloy in the T8 condition, which exhibited a tensile residual stress of +29 MPa, the graphene-reinforced composite in the same condition retained a compressive residual stress of −23 MPa. This represents a net improvement of 52 MPa, highlighting the composite's superior capability to retain compressive residual stress. The presence of graphene significantly influenced the stress distribution by introducing thermal expansion mismatch and acting as a barrier to dislocation motion. Overall, the composite demonstrated enhanced residual stress characteristics, making it a promising candidate for lightweight, fatigue-resistant aerospace components.

Keywords: AA2195 aluminum alloy; graphene reinforcement; hot rolling; residual stresses

Received: 15 June 2025
Revised: 14 July 2025
Accepted: 15 July 2025
Published: 16 July 2025

Citation: Manokaran, V.; Michael, A.X.; Pazhani, A.; Batako, A. Residual Stress Evolution of Graphene-Reinforced AA2195 (Aluminum–Lithium) Composite for Aerospace Structural Hydrogen Fuel Tank Application. *J. Compos. Sci.* **2025**, *9*, 369. https://doi.org/10.3390/jcs9070369

1. Introduction

In the pursuit of advanced lightweight materials for aerospace and space exploration applications, aluminum–lithium (Al–Li) alloys have emerged as promising candidates due to their high specific strength, excellent fatigue resistance, and superior corrosion behavior. Among them, AA2195, a third-generation Al–Li–Cu–Mg–Zr alloy, is widely recognized for its superior mechanical properties and low density, making it particularly suitable for structural components such as fuel tanks, cryogenic storage vessels, and load-bearing panels in launch vehicles. AA2195 has been extensively used in the fabrication of external

hydrogen fuel tanks for aerospace applications, notably due to its excellent performance under cryogenic conditions and the cyclic loading environments experienced during fuel pressurization and launch. While the current study was conducted under ambient conditions, the experimental insights are directly relevant to such service applications, as residual stress plays a critical role in determining the long-term mechanical integrity and dimensional stability of these structures under extreme operational environments. Specifically, residual stresses can influence fatigue performance, thermal mismatch behavior at cryogenic temperatures, and resistance to stress corrosion cracking—all of which are crucial considerations for hydrogen fuel tank materials [1,2]. To further enhance the performance of AA2195, recent studies have explored the incorporation of high-strength nanoscale reinforcements into the aluminum matrix. Graphene, a two-dimensional carbon nanomaterial, has gained significant attention due to its exceptional mechanical (~1 TPa Young's modulus), thermal (~5000 W/m·K conductivity), and electrical properties. When uniformly dispersed, graphene serves as an effective load-bearing and dislocation-blocking phase in metal matrix composites (MMCs), improving mechanical strength, wear resistance, and thermal behavior [3,4]. However, achieving uniform dispersion and strong interfacial bonding between graphene and the aluminum matrix remains a significant challenge [5,6]. A graphene content of 0.5 wt.% in the aluminum matrix composite has been shown to ensure uniform dispersion without agglomeration, resulting in improved mechanical properties. Conversely, adding more than 0.5 wt.% graphene tends to cause agglomeration, which adversely affects the mechanical strength. Therefore, 0.5 wt.% is considered the threshold limit for enhancing the mechanical performance of aluminum metal matrix composites [7,8]. In this study, a 0.5 wt.% graphene-reinforced AA2195 composite was fabricated using the squeeze casting technique, which promotes good wetting, minimal porosity, and uniform particle distribution. The cast composite was subjected to multi-pass hot rolling, followed by a T8 heat treatment cycle comprising solution treatment, cold rolling, and artificial aging, to refine the microstructure and enhance mechanical behavior [9]. The residual stress evolution was systematically evaluated after each stage of processing, including all rolling passes and thermal treatments. Residual stresses in aerospace-grade materials arise due to thermal gradients, plastic deformation, and phase transformations during processing. These internal stresses can significantly affect the structural performance [10]. Compressive residual stresses are desirable, as they inhibit crack initiation and propagation, thereby extending the fatigue life and improving dimensional stability—particularly beneficial for cyclic and cryogenic applications like hydrogen fuel tanks. In contrast, tensile residual stresses can lead to distortion, premature failure, or stress corrosion cracking [11,12]. In this work, the development of compressive residual stresses was attributed to thermal expansion mismatch between graphene and the aluminum matrix, combined with dislocation accumulation and microstructural constraints induced by the graphene particles. The formation of T_1 (Al_2CuLi) and θ' (Al_2Cu) precipitates during artificial aging also contributed to stress relaxation and mechanical strengthening [13]. The novelty of this study lies in its comprehensive analysis of residual stress behavior in a graphene-reinforced AA2195 alloy subjected to the complete T8 processing route. Although the experiments were conducted at room temperature, the findings are relevant for applications involving hydrogen storage at cryogenic temperatures and under cyclic loading conditions, as they provide fundamental insights into the internal stress evolution and stability in a high-performance aerospace composite. This research highlights the potential of graphene as a multifunctional reinforcement for next-generation hydrogen fuel tank materials in aerospace systems.

2. Materials and Methods

2.1. Fabrication of AA2195–Graphene Composite

In this study, the AA2195 aluminum alloy was used as the matrix material, and graphene nanoplatelets (0.5 wt.%) were selected as the reinforcement due to their exceptional mechanical and thermal properties. The composite was fabricated using the squeeze casting technique, which is known for producing high-quality metal matrix composites with minimal porosity and excellent mechanical integrity. To achieve a homogeneous dispersion of graphene within the AA2195 matrix, a two-step processing strategy was employed. In the first step, a powder mixture comprising 0.5 wt.% graphene nanoplatelets and 20 g of AA2900 aluminum alloy powder was prepared and subjected to high-energy ball milling for 1 h. The AA2900 alloy was deliberately chosen due to its chemical composition closely matching that of AA2195, thereby ensuring compositional compatibility and avoiding significant chemical mismatch during final consolidation. This compatibility is essential to prevent the formation of undesirable intermetallic phases or chemical inhomogeneity in the composite. Moreover, the AA2900 powder acted as a carrier medium for the graphene, enabling its uniform dispersion throughout the AA2195 melt during casting [9]. The blended powder was subsequently introduced into the molten AA2195 alloy, which was melted in a graphite crucible using an induction furnace under an inert argon atmosphere to prevent oxidation. The melt temperature was maintained at approximately 750 °C to ensure complete melting of the alloy and effective wetting of graphene particles. Mechanical stirring was performed at 500 rpm for 10 min to enhance the uniform distribution of graphene within the molten matrix. The resulting mixture was poured into a preheated steel die (maintained at 250 °C) that was integrated into the squeeze casting setup. A squeeze pressure of 110 MPa was immediately applied using a hydraulic press and maintained until complete solidification was achieved. The solidified ingot was then carefully removed and sectioned for further processing and characterization. This fabrication method yielded a dense, defect-free composite with uniform graphene dispersion, as confirmed by Energy-Dispersive X-ray Spectroscopy (EDS) analysis.

2.2. Hot Rolling Process

The graphene-reinforced AA2195 composite ingots were cut to dimensions of $50 \times 50 \times 12$ mm^3 using wire electrical discharge machining (WEDM) to meet the requirements for the hot rolling process. Rolling was carried out using the New Field Laboratory Rolling Machine, manufactured by New Field Engineers Pvt. Ltd., Mumbai, India, which is equipped with top and bottom rollers, each having a diameter of 105 mm. The rolling speed was maintained at 10 revolutions per minute (rev/min), and the applied rolling force was 1 N/mm. The composite was hot-rolled through four successive passes, followed by a single cold rolling pass, in accordance with the T8 heat treatment cycle adopted for the AA2195 composite, as illustrated in Figure 1.

Prior to each hot rolling pass, the samples were reheated to 480 °C, a temperature selected based on the recrystallization threshold of the aluminum alloy. This ensured adequate ductility, enabling plastic deformation while minimizing work hardening, cracking, and delamination. Reheating between passes promoted effective grain refinement and a uniform strain distribution and reduced the likelihood of rolling defects [14]. After hot rolling, the composite underwent solution treatment at 530 °C for 90 min to dissolve soluble phases and homogenize the microstructure. Subsequently, a single-pass cold rolling operation with minor thickness reduction was performed to introduce additional strain, preparing the material for artificial aging, in line with the T8 heat treatment sequence (solution treatment → cold working → artificial aging) [15]. The percentage elongation was measured in both the rolling direction and the transverse direction, yielding values of 10%

and 8%, respectively. The overall thickness reduction achieved was 4%. The detailed rolling pass parameters used during the hot and cold rolling processes of the AA2195–graphene composite are presented in Table 1.

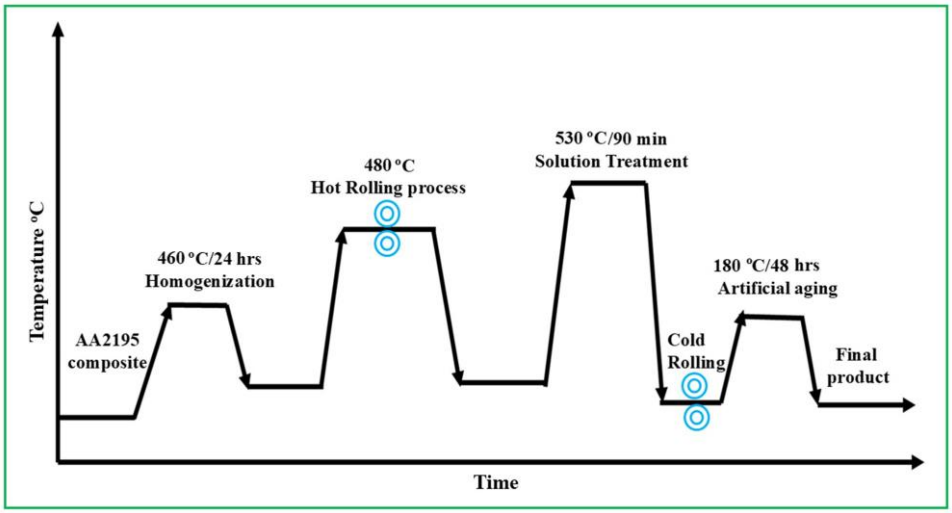

Figure 1. T8 heat treatment cycle adopted for AA2195–graphene composite.

Table 1. Rolling pass entrance and exit parameters.

Rolling Pass	1st	2nd	3rd	4th	Solution Treatment	5th
Entrance (mm)	12	11.9	11.8	11.7		11.6
Exit (mm)	11.9	11.8	11.7	11.6		11.5

2.3. Residual Stress Analysis

Residual stress analysis plays a vital role in understanding the internal stress distribution within advanced metal matrix composites, particularly in high-performance aerospace alloys such as AA2195 reinforced with graphene. During various manufacturing stages—including squeeze casting, hot rolling, and T8 heat treatment—residual stresses are inevitably introduced into the material. These stresses, which can be either tensile or compressive in nature, arise due to factors such as thermal gradients, phase transformations, differential plastic deformation, and the mismatch in thermal expansion between the matrix and reinforcement phases [16]. In the present investigation, a residual stress evaluation was carried out to characterize the stress state of the composite and to assess the influence of processing and graphene reinforcement on the material's structural integrity and performance. Surface-level residual stress measurements were conducted using a Pulstec μ-X360n portable X-ray residual stress analyzer, manufactured by Pulstec Industrial Co., Ltd., Hamamatsu, Japan. The analyzer has an effective X-ray penetration depth of approximately 8–10 μm in aluminum alloys. For each processing condition, measurements were repeated three times to ensure repeatability and statistical reliability. The average values obtained from these measurements are reported and further discussed in the present study. This system operates based on the cos α method—a non-destructive technique that is capable of providing rapid, precise, and real-time measurements directly on the material surface without altering the specimen. The analyzer's portability, accuracy, and ability to generate 2D stress maps make it particularly well-suited for in situ evaluations in laboratory environments. In this study, the single-incident angle method was employed using a chromium (Cr) target X-ray tube, which is standard for aluminum-based alloys. This

setup enabled the detection of the residual stress distributions on the surface, although the measurements were limited to surface layers due to equipment constraints. The measured residual stresses—whether tensile or compressive—can be attributed to the synergistic effects of hot working, thermal contraction upon cooling, and the dispersion of graphene particles, which act as effective barriers to dislocation movement. These factors collectively contribute to the development and redistribution of internal stresses within the composite matrix. Thus, residual stress analysis not only validates the mechanical stability of the developed composite but also provides essential insights for further process optimization and structural applications in aerospace components, where stress control is critical for long-term performance and reliability [17]. Figure 2a presents the Pulstec μ-X360n portable X-ray residual stress analyzer used in this study, and Figure 2b depicts the focusing point of the X-ray beam on the surface of the graphene-reinforced AA2195 composite sample.

Figure 2. (**a**) Pulstec μ-X360n, a portable X-ray residual stress analyzer; (**b**) X-ray beam on the surface of the graphene-reinforced AA2195 composite sample.

3. Result and Discussion

3.1. Microstructural Analysis of the Fabricated Composite

The fabricated composites were subjected to Scanning Electron Microscopy (SEM) to examine their microstructural features. Additionally, Energy-Dispersive Spectroscopy (EDS) was used to obtain accurate information on the elemental composition in both the as-cast and T8 heat-treated samples.

Figure 3a shows the SEM image of the AA2195–graphene composite in the as-cast condition, revealing a dendritic microstructure that is typically formed during solidification. The surface morphology displays a network of primary and secondary dendrite arms with relatively smooth grain boundaries. The microstructure also exhibits a uniform dispersion of graphene particles within the aluminum matrix, appearing as fine dark spots, which indicates the successful embedding of the reinforcement. Furthermore, no casting defects were observed in the composite, confirming the effectiveness of the squeeze casting process in producing a high-quality material. The presence of graphene appears to promote grain refinement and structural uniformity, thereby enhancing the overall quality of the composite. Figure 3b shows the corresponding EDS analysis of the as-cast sample, confirming the presence of the respective alloying elements of AA2195, along with a distinct carbon peak, attributed to the graphene reinforcement. Furthermore, Figure 3c shows the elemental mapping, which demonstrates the homogeneous dispersion of graphene across the scanned region. This confirms that the novel powder mixture is an effective method for achieving uniform graphene dispersion within the matrix [9,18].

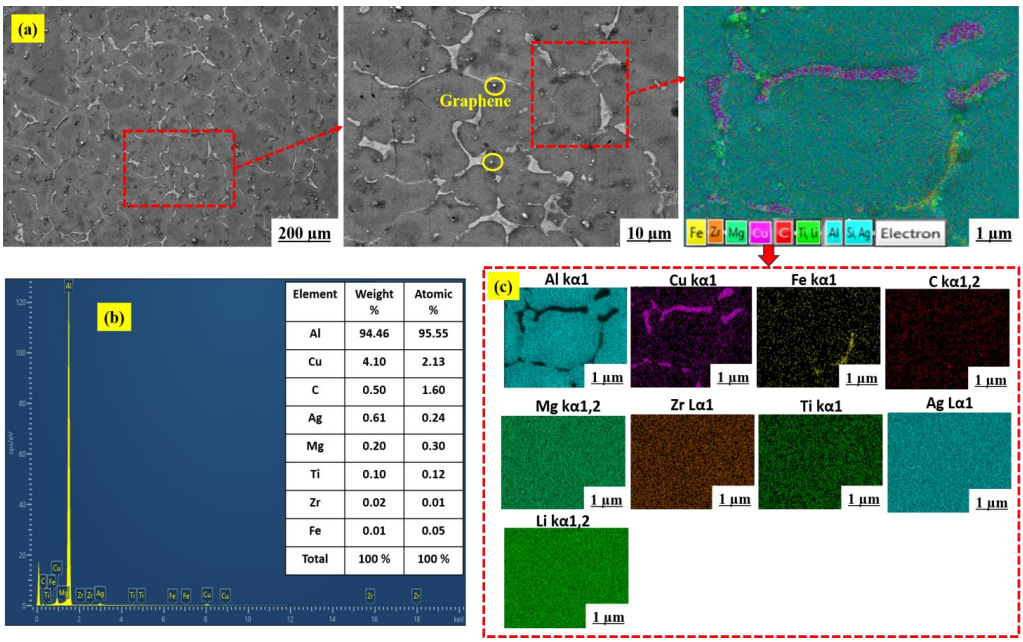

Figure 3. SEM analysis of the AA2195–graphene composite in the as-cast condition: (**a**) surface morphology, (**b**) EDS spectrum, and (**c**) elemental mapping.

Figure 4a presents the SEM image of the AA2195–graphene composite in the hot-rolled and T8 heat-treated condition, which shows a significant transformation in microstructural features compared to the as-cast state. The microstructure reveals refined aluminum grains, and the graphene particles remain uniformly dispersed within the matrix. Additionally, needle-shaped fine precipitates, such as T1 (Al_2CuLi) and θ′ (Al_2Cu) phases, can be observed, as highlighted by the red box in the SEM micrographs. These nanoscale features are uniformly distributed both within the grains and along the grain boundaries, having precipitated during the artificial aging process conducted at 180 °C. These precipitates contribute significantly to the enhanced mechanical properties by impeding dislocation movement and improving interfacial bonding between the matrix and the reinforcement. The uniform distribution of graphene, along with the presence of strengthening precipitates, demonstrates the effectiveness of the combined thermomechanical and aging treatments in refining the microstructure and enhancing the overall performance of the composite [19,20]. Figure 4b shows the corresponding EDS analysis of the hot-rolled and T8 heat-treated samples. The analysis indicates the presence of the major alloying elements of AA2195, along with a uniform distribution of graphene particles. The consistent intensity and distribution of these elemental peaks confirm that the chemical composition remains stable and well-integrated after thermomechanical processing. The presence of carbon peaks verifies the successful retention and uniform dispersion of graphene sheets within the matrix, even after exposure to high temperatures and mechanical deformation. Additionally, Figure 4c shows the EDS mapping, which confirms the homogeneous distribution of elements across the scanned area, indicating that no significant segregation or agglomeration occurred during the rolling or aging processes.

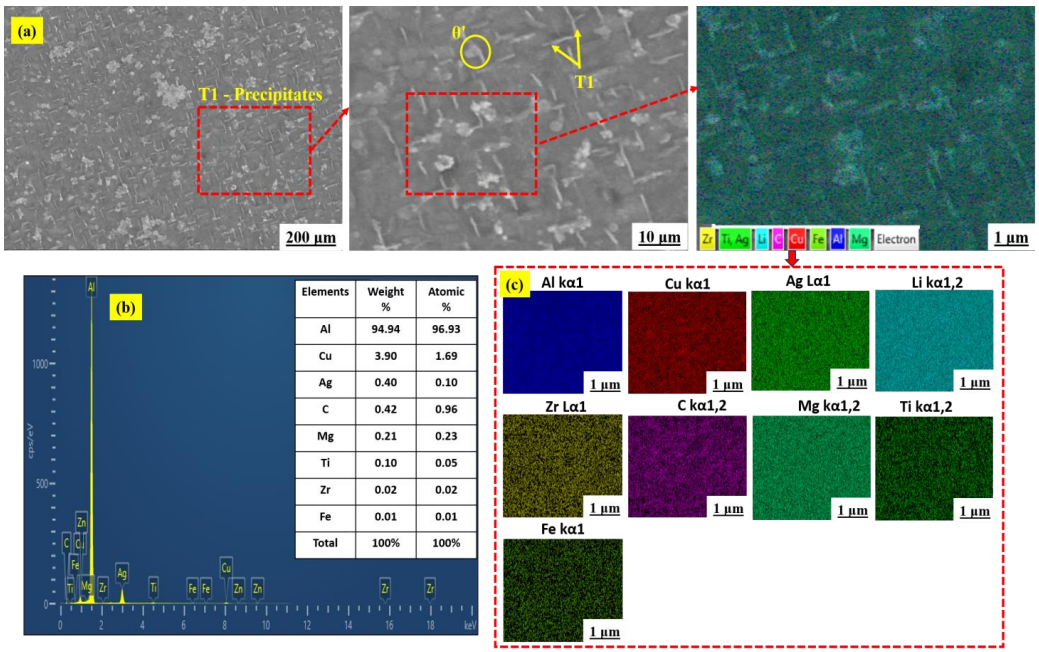

Figure 4. SEM analysis of the AA2195–graphene composite in the hot-rolled T8 condition: (**a**) surface morphology, (**b**) EDS spectrum, and (**c**) elemental mapping.

3.2. Residual Stress Analysis of AA2195 in the As-Received Condition

The residual stress of the unreinforced (pure) AA2195 alloy was measured in the as-procured ingot, which had been processed in accordance with the T8 heat treatment cycle. The measured residual stress, as shown in Figure 5, was 29 MPa and primarily tensile in nature. This tensile stress is mainly attributed to the thermal contraction mismatch during the quenching phase of the T8 heat treatment. During rapid cooling after solution heat treatment, the outer regions of the alloy contract more rapidly than the inner core, leading to the development of surface tensile stresses. Furthermore, in the absence of reinforcing particles such as graphene, there are no effective internal barriers to dislocation movement, allowing tensile residual stresses to persist without significant relaxation or redistribution [21].

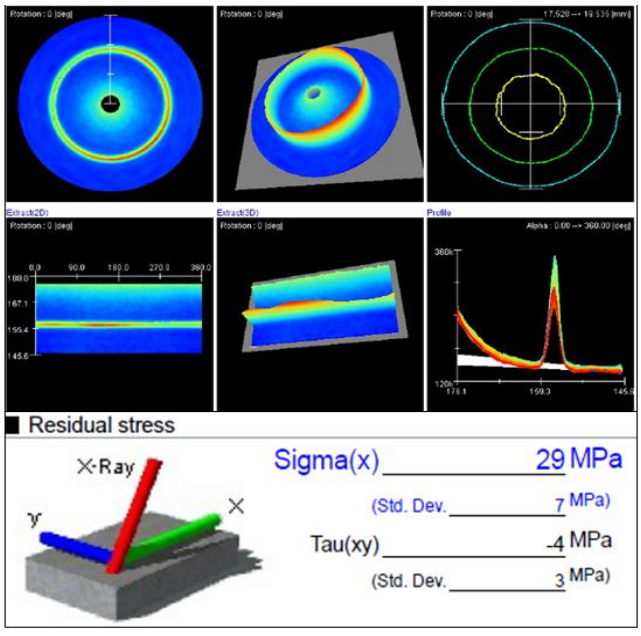

Figure 5. Residual stress distribution map of AA2195 in the as-procured condition.

3.3. Residual Stress Analysis of AA2195–Graphene Composite in the As-Cast Condition

Figure 6 shows the residual stress distribution map of the graphene-reinforced AA2195 composite in the as-cast condition. The measured residual stress was −24 MPa, indicating a primarily compressive nature. Compared to the unreinforced (pure) AA2195 alloy, which exhibited a tensile residual stress of 29 MPa, the composite shows a notable reduction and reversal in the residual stress state. This transition from tensile to compressive residual stress is primarily influenced by the presence of uniformly dispersed graphene particles, which alter the stress evolution by impeding dislocation mobility and promoting a more uniform strain distribution during solidification [22]. Furthermore, the mismatch in the coefficient of thermal expansion (CTE) between the aluminum matrix and the graphene reinforcement leads to the development of internal compressive stresses upon cooling. The graphene particles also contribute to localized constraint within the microstructure, promoting a more uniform and stable residual stress distribution. Such compressive residual stresses are generally beneficial to the composite's performance, as they can enhance fatigue resistance, delay crack initiation, and improve the overall dimensional stability, especially under cyclic loading conditions [23,24].

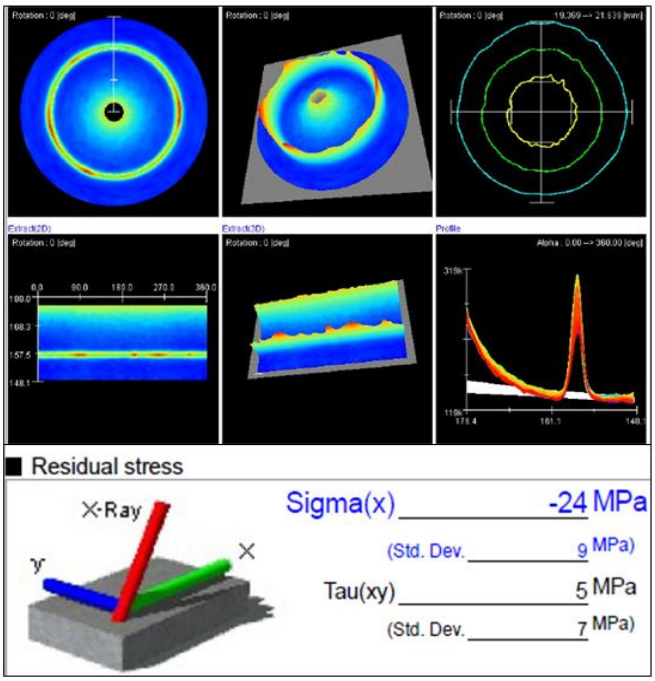

Figure 6. Residual stress distribution map of the AA2195–graphene composite in the as-cast condition.

3.4. Residual Stress Analysis of AA2195–Graphene Composite After First Pass of Hot Rolling

After the first pass of hot rolling, which reduced the composite thickness from 12 mm to 11.9 mm, a compressive residual stress of –31 MPa was recorded, as shown in Figure 7. This stress primarily arises from the mismatch in thermal expansion coefficients and plastic deformation behavior between the AA2195 matrix and the 2D graphene reinforcement. The slight thickness reduction induced localized plastic strain, resulting in compressive stress near the surface. Such compressive residual stresses are generally beneficial, as they enhance the fatigue resistance and delay crack initiation. Prior to hot rolling, the AA2195–graphene composite was homogenized at 460 °C for 24 h, in accordance with the T8 heat treatment cycle. This homogenization step was essential for eliminating elemental segregation and promoting a uniform microstructure. It facilitated the diffusion of solute atoms such as Cu and Li, which are necessary for the formation of T1 (Al_2CuLi) and θ′ (Al_2Cu) precipitates during subsequent aging [25]. Moreover, the process improved the

thermal stability and dispersion of the 0.5 wt.% graphene particles within the aluminum matrix, preventing agglomeration and enabling effective load transfer during deformation. By achieving a homogenized and supersaturated solid solution, the composite was optimally prepared for hot rolling, which would further refine the grain structure and activate key strengthening mechanisms. As the rolling progresses through successive passes, the magnitude of the compressive residual stress near the surface is expected to increase. However, due to inhomogeneous plastic deformation and work hardening, the core may experience a transition to tensile stress. Tracking the evolution of residual stresses after each pass is therefore critical to understanding stress redistribution and its implications for the dimensional stability and mechanical performance of the final rolled composite [26].

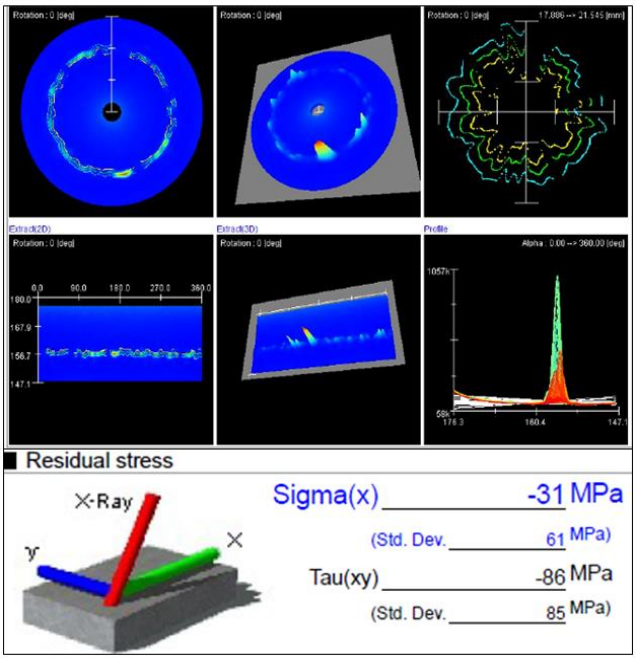

Figure 7. Residual stress distribution map of the AA2195–graphene composite after the first pass of hot rolling.

3.5. Residual Stress Analysis of AA2195–Graphene Composite After Second Pass of Hot Rolling

Following the second hot rolling pass, the composite thickness was further reduced from 11.9 mm to 11.8 mm. At this stage, the residual stress was measured to be −32 MPa, as shown in Figure 8, indicating a slight increase in compressive stress compared to the first pass. This incremental rise is primarily attributed to the accumulation of localized plastic strain and the progressive work hardening of the matrix due to continued deformation [27]. Despite the minimal thickness reduction, the repeated rolling action continues to densify dislocations and enhance the interaction between graphene particles and the surrounding aluminum lattice. The persistence of surface compressive residual stress remains beneficial—particularly in suppressing crack initiation, improving fatigue performance, and maintaining surface integrity during the early stages of deformation. Moreover, the graphene reinforcement continues to play a pivotal role in stabilizing dislocations and hindering grain boundary migration. As additional hot rolling passes are applied, further residual stress redistribution is expected—especially between the surface and core regions—due to evolving strain gradients and differential constraint effects across the composite's thickness. Monitoring these stress transitions is essential for understanding the mechanical response, structural reliability, and dimensional stability of the rolled composite plate [28].

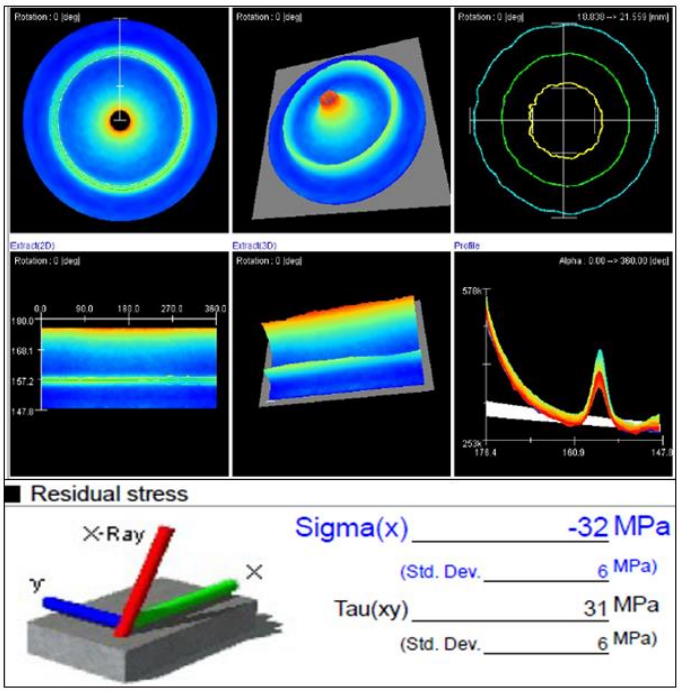

Figure 8. Residual stress distribution map of the AA2195–graphene composite after the second pass of hot rolling.

3.6. Residual Stress Analysis of AA2195–Graphene Composite After Third Pass of Hot Rolling

Following the third pass of hot rolling, the composite thickness was further reduced from 11.8 mm to 11.7 mm. Despite the relatively small reduction in thickness, a compressive residual stress of –36 MPa was recorded, as shown in Figure 9, representing a noticeable increase compared to the previous pass. This increment highlights the cumulative effect of progressive plastic deformation and the internal stress fields that are introduced by the stiff 2D graphene reinforcement. The uniformly dispersed graphene particles within the aluminum matrix act as pinning sites at grain boundaries, effectively limiting grain growth and restricting dislocation movement. This constraint leads to the accumulation of internal stresses, which manifest as compressive residual stresses near the surface. Moreover, the mismatch in mechanical properties between graphene and the aluminum alloy matrix induces internal constraints during deformation, further contributing to stress buildup. This observed increase in compressive residual stress, despite minimal thickness reduction, underscores the role of graphene in enhancing the material's response to rolling-induced deformation [29]. The interaction between dislocations and graphene reinforcements facilitates strain hardening and promotes a more favorable compressive stress state, which can positively influence fatigue resistance and dimensional stability in the final rolled composite [30].

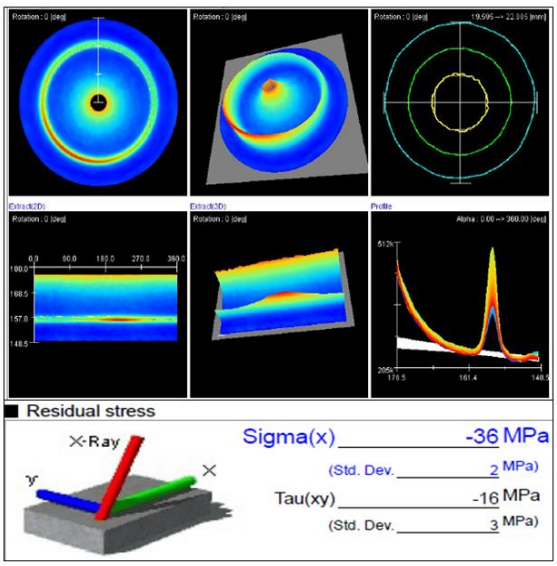

Figure 9. Residual stress distribution map of the AA2195–graphene composite after the third pass of hot rolling.

3.7. Residual Stress Analysis of AA2195–Graphene Composite After Fourth Pass of Hot Rolling

After the fourth hot rolling pass, the composite thickness was reduced from 11.7 mm to 11.6 mm. A substantial increase in compressive residual stress was observed at this stage, reaching –68 MPa, as shown in Figure 10.

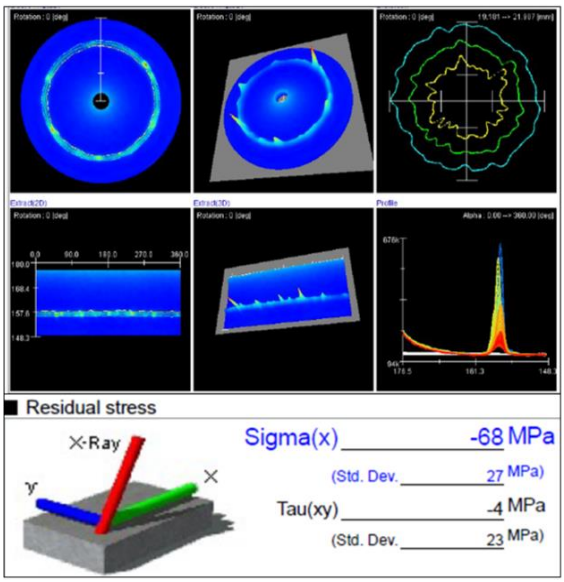

Figure 10. Residual stress distribution map of the AA2195–graphene composite after the fourth pass of hot rolling.

This sharp rise, despite the minor thickness reduction, is primarily attributed to the cumulative plastic strain that accumulated during the previous passes, the significantly increased dislocation density, and the strong pinning effect exerted by the uniformly dispersed graphene particles. By the fourth pass, extensive work hardening had occurred, markedly increasing the internal dislocation density. The combination of this high dislocation content and the effective barriers posed by the graphene reinforcements severely restricted dislocation mobility. As a result, deformation became increasingly localized around the graphene particles, intensifying the buildup of internal compressive stress [31]. Moreover, as rolling progresses, strain tends to concentrate near the surface layers—where residual stresses are typically

measured—leading to a disproportionate increase in compressive stress. The mechanical mismatch between the hardened aluminum matrix and the stiff graphene sheets further amplifies resistance to deformation, thereby promoting additional stress development. Thus, the steep increase in residual stress is not solely a consequence of geometric thickness reduction but is instead the result of the nonlinear accumulation of plastic strain, intensified work hardening, and interfacial constraints imposed by the graphene reinforcement—collectively reaching a critical threshold during this stage of rolling [32].

3.8. Residual Stress Analysis of AA2195–Graphene Composite After Fifth Pass of Cold Rolling

Before the fifth pass, the composite underwent solution treatment at 530 °C in accordance with the T8 heat treatment cycle. This step was introduced not only to dissolve coarse pre-existing precipitates and bring alloying elements such as copper and lithium into the solid solution, but also to relieve the residual stresses that had accumulated during the preceding hot rolling passes. The solution treatment enhanced the composite's ductility and workability, thereby preparing it for the final deformation stage. Following solution treatment, the composite was rapidly quenched in water to retain a supersaturated solid solution [33].

The fifth pass was then carried out under cold rolling conditions, reducing the composite thickness from 11.6 mm to 11.5 mm. This cold deformation introduced additional strain hardening and a notable increase in the dislocation density. These dislocations subsequently act as effective nucleation sites for the formation of fine, strengthening precipitates during the artificial aging process [8,34]. Interestingly, after the fifth pass, the measured compressive residual stress decreased from −68 MPa to −40 MPa, as shown in Figure 11. This reduction is primarily attributed to the stress-relieving effect of the high-temperature solution treatment conducted prior to cold rolling. During the solution treatment, a substantial portion of the internal stresses that were generated in the earlier hot rolling stages was relaxed. Although cold rolling typically contributes to dislocation multiplication and additional strain, the relatively small thickness reduction in this pass, combined with the improved ductility and uniform deformation characteristics at room temperature, limited the buildup of residual stress. Moreover, cold rolling promoted a more homogeneous strain distribution, thereby reducing localized strain concentrations that would otherwise elevate residual stress levels [35].

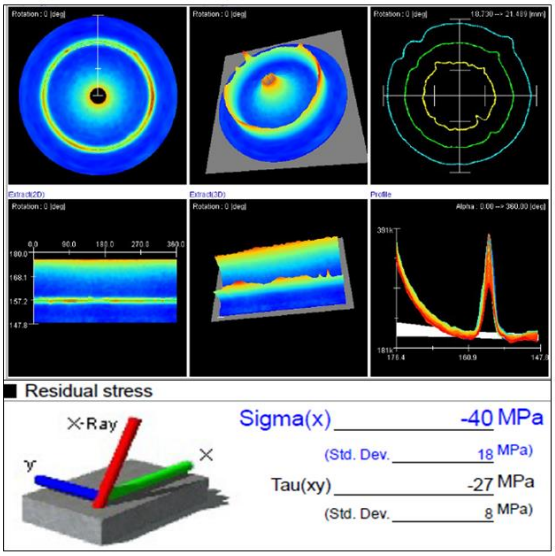

Figure 11. Residual stress distribution map of the AA2195–graphene composite after the fifth pass of cold rolling.

3.9. Residual Stress Analysis of AA2195–Graphene Composite in the Artificially Aged (T8) Condition

Following the fifth pass of cold rolling, the AA2195–graphene composite was subjected to artificial aging at 180 °C for 48 h in accordance with the T8 heat treatment cycle. During this stage, fine and uniformly distributed precipitates—primarily T_1 (Al_2CuLi) and θ′ (Al_2Cu)—were formed, significantly enhancing the mechanical strength of the composite [19]. Compared to the cold-rolled condition after the fifth pass, the residual compressive stress in the artificially aged condition (180 °C for 48 h) decreased by 17 MPa, dropping from –40 MPa to –23 MPa, as shown in Figure 12.

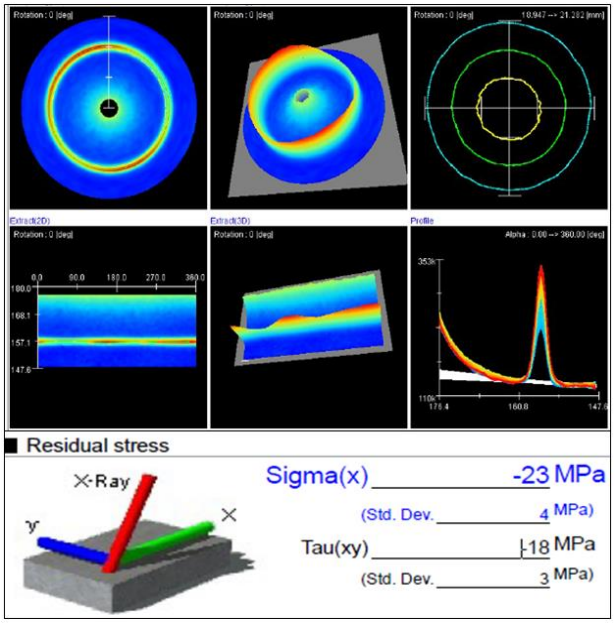

Figure 12. Residual stress distribution map of the AA2195–graphene composite in the artificially aged T8 condition.

This reduction is primarily attributed to the recovery of dislocation structures and the activation of stress relaxation mechanisms during artificial aging. These thermally driven processes alleviate internal stresses induced by prior cold deformation while retaining the microstructural strengthening effects associated with work hardening and dislocation density [36]. The precipitation of T_1 and θ′ phases further contribute to microstructural stabilization, supporting both mechanical strength and stress relief. When compared to the unreinforced AA2195 alloy in the T8 condition, the graphene-reinforced composite retains a compressive residual stress state. This compressive nature is primarily the result of the addition of 0.5 wt.% graphene particles, which introduce a significant thermal expansion mismatch between the aluminum matrix and the graphene reinforcement during cooling after solution treatment and aging [9,37]. Graphene possesses a much lower coefficient of thermal expansion (CTE) compared to aluminum. During the post-aging cooling, the greater contraction of the aluminum matrix relative to the embedded graphene particles leads to the development of compressive residual stresses around the reinforcement. Additionally, graphene serves as a strong barrier to dislocation motion and acts to pin grain boundaries, both of which contribute to the accumulation and retention of compressive stress within the matrix. This residual compressive stress is advantageous for the composite's performance, as it enhances fatigue resistance and suppresses crack initiation under cyclic loading—properties that are especially critical for aerospace structural applications [38,39].

4. Conclusions

- A novel 0.5 wt.% graphene-reinforced AA2195 composite was successfully fabricated using squeeze casting, followed by multi-pass hot rolling and T8 heat treatment, resulting in a homogeneously strengthened aluminum matrix composite.
- Microstructural analysis of SEM images confirmed the uniform distribution of graphene particles within the AA2195 matrix, accompanied by significant grain refinement and the formation of fine precipitates such as θ′ (Al_2Cu) and T1 (Al_2CuLi).
- The addition of graphene particles significantly influenced the residual stress behavior of the composite. The final stage of the T8 condition exhibited compressive residual stress (−23 MPa), in contrast to the parent alloy, due to the thermal expansion mismatch and interfacial constraint effects induced by graphene.
- Throughout the rolling passes, residual stress was carefully monitored. The fifth pass, conducted under cold rolling conditions, increased the strain hardening and dislocation density, which subsequently relaxed during artificial aging. The overall reduction in residual stress (from −68 MPa to −23 MPa) confirmed effective stress stabilization without compromising strength.
- Compared to the unreinforced parent alloy, the graphene-reinforced AA2195 composite exhibited enhanced compressive residual stress characteristics, making it a promising candidate for lightweight, high-strength aerospace applications, especially in components that are subjected to cyclic loading and fatigue.

Author Contributions: V.M., Conceptualization, Investigation, Formal analysis, and Writing—original draft. A.P., Resources, Data curation, Project administration, and Supervision. A.B., and A.X.M., Methodology, Supervision, Validation, Visualization, and Writing—review and editing. All authors have read and agreed to the published version of the manuscript.

Funding: The authors received no external funding for this research.

Data Availability Statement: The data supporting the findings of this study are available from the corresponding author upon reasonable request.

Acknowledgments: The authors gratefully acknowledge Vellore Institute of Technology (VIT), Vellore, for providing the necessary facilities and infrastructure to carry out this research work.

Conflicts of Interest: The authors declare that they have no known competing financial interests or personal relationships that could have appeared to influence the work reported in this paper.

References

1. Hajjioui, E.A.; Bouchaâla, K.; Faqir, M.; Essadiqi, E. A Review of Manufacturing Processes, Mechanical Properties and Precipitations for Aluminum Lithium Alloys Used in Aeronautic Applications. *Heliyon* **2023**, *9*, e12565. [CrossRef] [PubMed]
2. Eswara Prasad, N.; Gokhale, A.A.; Wanhill, R.J.H. Aluminium–Lithium Alloys. In *Aerospace Materials and Material Technologies*; Springer: Singapore, 2017; Volume 1, pp. 53–72.
3. Chen, W.; Yang, T.; Dong, L.; Elmasry, A.; Song, J.; Deng, N.; Elmarakbi, A.; Liu, T.; Lv, H.B.; Fu, Y.Q. Advances in Graphene Reinforced Metal Matrix Nanocomposites: Mechanisms, Processing, Modelling, Properties and Applications. *Nanotechnol. Precis. Eng.* **2020**, *3*, 189–210. [CrossRef]
4. Liu, J.; Zhang, Y.; Zhang, H.; Yang, J. Mechanical Properties of Graphene-Reinforced Aluminium Composite with Modified Substrate Surface: A Molecular Dynamics Study. *Nanotechnology* **2021**, *32*, 085712. [CrossRef] [PubMed]
5. Ghodrati, H.; Ghomashchi, R. Effect of Graphene Dispersion and Interfacial Bonding on the Mechanical Properties of Metal Matrix Composites: An Overview. *FlatChem* **2019**, *16*, 100113. [CrossRef]
6. Hu, Z.; Wu, Z.; Luo, S.; Wang, X.; Nian, Q.; Chen, Y.; Nagaumi, H. Large Scale Production of Graphene Aluminum Composites by Stir Casting: Process, Microstructure and Properties. *J. Mater. Res. Technol.* **2023**, *27*, 681–691. [CrossRef]
7. Lou, S.M.; Qu, C.D.; Guo, G.X.; Ran, L.W.; Liu, Y.Q.; Zhang, P.P.; Su, C.J.; Wang, Q.B. Effect of Fabrication Parameters on the Performance of 0.5 Wt.% Graphene Nanoplates-Reinforced Aluminum Composites. *Materials* **2020**, *13*, 3483. [CrossRef] [PubMed]

8. Venkatraman, M.; Xavior, M.A. Microstructural Study and Property Evaluation of Graphene Reinforced AA2195 Metal Matrix Composites. *Results Eng.* **2025**, *25*, 104492. [CrossRef]
9. Ashwath, P.; Venkatraman, M.; Patel, A.; Xavior, M.A.; Batako, A. Innovation in Sustainable Composite Research: Investigating Graphene-Reinforced MMCs for Liquid Hydrogen Storage Tanks in Aerospace and Space Exploration. *J. Mater. Res. Technol.* **2024**, *33*, 4313–4331. [CrossRef]
10. Withers, P.J.; Bhadeshia, H.K.D.H. Residual Stress. Part 2—Nature and Origins. *Mater. Sci. Technol.* **2001**, *17*, 366–375. [CrossRef]
11. Hosseini, S.; Farajollahi, M.; Ebrahimi, M. Residual Stress, Fatigue Behavior, and Mechanical Properties of Equal-Channel Angular Pressed Commercial Pure Titanium. *J. Mater. Res. Technol.* **2024**, *28*, 3297–3305. [CrossRef]
12. Wong, C.S.; Pramanik, A.; Basak, A.K. Residual Stress Generation in Metal Matrix Composites after Cooling. *Mater. Sci. Technol.* **2018**, *34*, 1388–1400. [CrossRef]
13. Wang, X.; Rong, Q.; Shi, Z.; Li, Y.; Cao, J.; Chen, B.; Lin, J. Investigation of Stress Effect on Creep, Precipitation and Dislocation Evolution of Al–Li Alloy during Creep Age Forming. *Mater. Sci. Eng. A* **2022**, *836*, 142723. [CrossRef]
14. Algendy, A.Y.; Rometsch, P.; Chen, X.-G. Impact of Hot Rolling Temperature on the Mechanical Properties and Microstructural Evolution of Hot/Cold-Rolled AA5083 with Sc and Zr Microalloying. *Mater. Sci. Eng. A* **2024**, *896*, 146275. [CrossRef]
15. Xu, X.; Wu, G.; Zhang, L.; Tong, X.; Zhang, X.; Sun, J.; Li, L.; Xiong, X. Effects of Heat Treatment and Pre-Stretching on the Mechanical Properties and Microstructure Evolution of Extruded 2050 Al–Cu–Li Alloy. *Mater. Sci. Eng. A* **2022**, *845*, 143236. [CrossRef]
16. Li, Y.; Gan, W.; Zhou, W.; Li, D. Review on Residual Stress and Its Effects on Manufacturing of Aluminium Alloy Structural Panels with Typical Multi-Processes. *Chin. J. Aeronaut.* **2023**, *36*, 96–124. [CrossRef]
17. Ammar, M.M.A.; Shirinzadeh, B.; Zhao, P.; Shi, Y. Optimization of Process-Induced Residual Stresses in Automated Manufacturing of Thermoset Composites. *Aerosp. Sci. Technol.* **2022**, *123*, 107443. [CrossRef]
18. Abd Rahim, M.N.; Salleh, M.S.; Yahaya, S.H.; Subramonian, S.; Jun, L.P.; Abdul Rashid, A.H.; Syed Ahmad, S.N.A.; Al-Zubaidi, S.S. Effect of Graphene Addition on Microstructure and Mechanical Properties of Cast Aluminium Alloy Composite. *J. Adv. Res. Micro Nano Eng.* **2024**, *25*, 66–75. [CrossRef]
19. Duan, S.; Liu, Z.; Guo, F.; Pan, Y.; Matsuda, K.; Zou, Y. Precipitates Evolution during Artificial Aging and Their Influence on Mechanical Properties of a Cast Al–Cu–Li Alloy. *J. Mater. Res. Technol.* **2023**, *22*, 2502–2517. [CrossRef]
20. Li, M.; Yang, W.; Tian, X.; Chen, L.; Hou, H.; Zhao, Y. Precipitation and Refining of Al2Cu in Graphene Nanoplatelets Reinforced 2024 Al Composites. *Mater. Charact.* **2023**, *200*, 112854. [CrossRef]
21. Zhang, Y.; Yi, Y.; Huang, S.; Dong, F. Influence of Quenching Cooling Rate on Residual Stress and Tensile Properties of 2A14 Aluminum Alloy Forgings. *Mater. Sci. Eng. A* **2016**, *674*, 658–665. [CrossRef]
22. Shokrieh, M.M.; Ghanei Mohammadi, A.R. 1 - The importance of measuring residual stresses in composite materials. In *Residual Stresses in Composite Materials*; Shokrieh, M.M., Ed.; Woodhead Publishing: Oxford, UK, 2014; pp. 3–14. ISBN 9780857092700. [CrossRef]
23. Teixeira-Dias, F.; Menezes, L.F. *Thermal Residual Stresses in Aluminium Matrix Composites*; Springer: Berlin/Heidelberg, Germany, 2010; pp. 33–62.
24. Iqbal, A.A.; Arai, Y.; Araki, W. Influence of Residual Stress on the Fatigue Crack Growth Mechanism in the Al-Alloy/Hybrid MMC Bi-Material. *J. Fail. Anal. Prev.* **2022**, *22*, 1468–1477. [CrossRef]
25. Huang, H.; Xiong, W.; Jiang, Z.; Zhang, J. A Quasi In-Situ Study on the Microstructural Evolution of 2195 Al-Cu-Li Alloy during Homogenization. *Materials* **2022**, *15*, 6573. [CrossRef] [PubMed]
26. Dixit, U.S.; Dixit, P.M. A Study on Residual Stresses in Rolling. *Int. J. Mach. Tools Manuf.* **1997**, *37*, 837–853. [CrossRef]
27. Withers, J.P.; Roy, J.M. 4.10 Residual Stresses in Metal Matrix Composites. In *Comprehensive Composite Materials II*; Beaumont, P.W.R., Zweben, C.H., Eds.; Elsevier: Oxford, UK, 2018; pp. 275–286. ISBN 9780081005347. [CrossRef]
28. Yang, Z.; Ni, Z.; Yan, J.; Fan, L.; Zhang, J.; Chen, X.; Guan, R. Towards High Performance Nano Multilayered Graphene/5052 Al Composite: In Situ Interfacial Tailoring via Accumulative Roll Bonding. *Carbon* **2025**, *238*, 120213. [CrossRef]
29. Mukherjee, S.; Ananth, C.R.; Chandra, N. Effect of Residual Stresses on the Interfacial Fracture Behavior of Metal-Matrix Composites. *Compos. Sci. Technol.* **1997**, *57*, 1501–1512. [CrossRef]
30. Yan, Y.; Zhao, J.; Chen, L.; Zhao, H.; Klimova-Korsmik, O.; Tolochko, O.V.; Yin, F.; Ji, P.; Kang, S. Effect of Strain Rate on Compressive Properties of Aluminium-Graphene Composites. *Metals* **2023**, *13*, 618. [CrossRef]
31. Wang, M.; Sheng, J.; Wang, L.-D.; Yang, Z.-Y.; Shi, Z.-D.; Wang, X.-J.; Fei, W.-D. Hot Rolling Behavior of Graphene/Cu Composites. *J. Alloys Compd.* **2020**, *816*, 153204. [CrossRef]
32. Yang, K.M.; Ma, Y.C.; Zhang, Z.Y.; Zhu, J.; Sun, Z.B.; Chen, J.S.; Zhao, H.H.; Song, J.; Li, Q.; Chen, N.Q.; et al. Anisotropic Thermal Conductivity and Associated Heat Transport Mechanism in Roll-to-Roll Graphene Reinforced Copper Matrix Composites. *Acta. Mater.* **2020**, *197*, 342–354. [CrossRef]
33. Jang, J.-H.; Nam, D.-G.; Park, Y.-H.; Park, I.-M. Effect of Solution Treatment and Artificial Aging on Microstructure and Mechanical Properties of Al–Cu Alloy. *Trans. Nonferrous Met. Soc. China* **2013**, *23*, 631–635. [CrossRef]

34. Zhou, C.; Zhan, L.; Liu, C.; Huang, M. Influence of Dislocation Morphology on T1 Precipitation of an Al-Cu-Li Alloy. *J. Alloys Compd.* **2023**, *947*, 169463. [CrossRef]
35. Rashidi, M.; Tayebi, P.; Hashemi, R. Stress Relief Treatment of Aluminum/Magnesium Laminates Fabricated by Roll Bonding Technique. *Heliyon* **2025**, *11*, e41639. [CrossRef] [PubMed]
36. Requena, G.; Yubero, D.C.; Corrochano, J.; Repper, J.; Garcés, G. Stress Relaxation during Thermal Cycling of Particle Reinforced Aluminium Matrix Composites. *Compos. Part A Appl. Sci. Manuf.* **2012**, *43*, 1981–1988. [CrossRef]
37. Xu, X.; Wu, G.; Zhang, L.; Tong, X.; Qi, F.; Guo, Y.; Li, L.; Xiong, X.; Wang, C. Regulation of Precipitation Behavior among T1, S′, and θ′ Phases in Al–Cu–Li-(Mg–Ag) Alloys by Optimizing Ag/Mg Ratios. *Mater. Sci. Eng. A* **2023**, *876*, 145158. [CrossRef]
38. Tsai, S.-D.; Mahulikar, D.; Marcus, H.L.; Noyan, I.C.; Cohen, J.B. Residual Stress Measurements on Al-Graphite Composites Using X-Ray Diffraction. *Mater. Sci. Eng.* **1981**, *47*, 145–149. [CrossRef]
39. Abd-Elaziem, W.; Khedr, M.; Elsheikh, A.H.; Liu, J.; Zeng, Y.; Sebae, T.A.; Abd El-Baky, M.A.; Darwish, M.A.; Daoush, W.M.; Li, X. Influence of Nanoparticles Addition on the Fatigue Failure Behavior of Metal Matrix Composites: Comprehensive Review. *Eng. Fail. Anal.* **2024**, *155*, 107751. [CrossRef]